Copy No. _____

Defence Research and Development Canada
Recherche et développement pour la défense Canada

DEFENCE R&D DÉFENSE

MEMS Based Acoustic Thermomechanical Characterization of Aluminum 6061-T651 Beams

Gino Rinaldi
NSERC Research Fellow

Defence R&D Canada – Atlantic

Technical Memorandum
DRDC Atlantic TM 2009-080
September 2009

Canada

This page intentionally left blank.

MEMS Based Acoustic Thermomechanical Characterization of Aluminum 6061-T651 Beams

Gino Rinaldi
NSERC Research Fellow

Defence R&D Canada – Atlantic

Technical Memorandum
DRDC Atlantic TM 2009-080
September 2009

Principal Author

Original signed by Gino Rinaldi

Gino Rinaldi

NSERC Research Fellow

Approved by

Original signed by Ken McRae

Ken McRae

Head / Air Vehicles Research Section

Approved for release by

Original signed by Ron Kuwahara for

Dr. Calvin V. Hyatt

Chief Scientist / DRDC Atlantic

Abstract

Temperature based testing is an important tool in determining the mechanical characteristics of structures. Metallic structures such as aluminum beams respond to high and low temperatures by expanding or contracting accordingly. Hence, the structure under goes changes in geometry that can influence its performance. Similarly, the elastic property of the material has a temperature dependence that contributes significantly to the overall mechanical qualities of the material. These thermally induced changes in geometrical and elastic parameters can be monitored through experimentation. In this work, a method based on flexural frequency response is described in which the variation in the experimental 5^{th} natural frequency under thermal loading is employed to extract the coefficient of thermal dependence of Young's modulus. This coefficient is then employed in the theoretical model to validate the experimental 2^{nd}, 3^{rd}, 4^{th} and 5^{th} natural frequencies of the aluminum beam. A micro-electro-mechanical-systems based microphone is used to monitor the frequency response of the vibrating beam. The theoretical model is based on a *free-free* boundary supported beam from which the natural frequencies are obtained. Constant geometry and constant elasticity models are also presented and compared. For demonstration purposes the proposed method is applied to an aluminum 6061-T651 beam. Experimental results are good agreement with the theoretical formulation.

Résumé

Les tests basés sur la température constituent un outil important pour la détermination des caractéristiques mécaniques de structures. Les structures métalliques, comme les poutres en aluminium, répondent aux températures basses ou élevées en se contractant ou en se dilatant. La structure subit donc des modifications de sa géométrie qui peuvent avoir une influence sur sa performance. De même, la propriété élastique du matériau est dépendante de la température, ce qui contribue de manière significative aux qualités mécaniques générales de celui-ci. Ces modifications des paramètres géométriques et élastiques induites par la température peuvent être suivies au moyen d'expériences. Dans le cas présent, on décrit une méthode basée sur la réponse en fréquence à la flexion pour laquelle la variation de la $5^{ème}$ fréquence naturelle expérimentale sous charge thermique est utilisée pour extraire le coefficient de dépendance thermique du module d'élasticité. Ce coefficient est ensuite utilisé avec le modèle théorique pour valider les $2^{ème}$, $3^{ème}$, $4^{ème}$ et $5^{ème}$ fréquences naturelles expérimentales de la poutre en aluminium. On utilise un microphone basé sur un système micro-électromécanique pour suivre la réponse en fréquence de la poutre vibrante. Le modèle théorique est basé sur une poutre soutenue à limites *libre-libre* à partir de la quelle on obtient les fréquences naturelles. On présente aussi des modèles à élasticité constante et à géométrie constante et on les compare. À des fins de démonstration, la méthode proposée est appliquée à une poutre en aluminium 6061-T651. Les résultats expérimentaux obtenus concordent bien avec la formulation théorique.

This page intentionally left blank.

Executive summary

MEMS Based Acoustic Thermomechanical Characterization of Aluminum 6061-T651 Beams

Rinaldi, G.; DRDC Atlantic TM 2009-080; Defence R&D Canada – Atlantic; September 2009.

Introduction or background

Temperature based testing is a valuable and important tool in determining the mechanical characteristics of structures. In this regard, metallic structures such as aluminum beams respond to high and low temperatures by expanding or contracting accordingly. The elastic property of aluminum 6061-T651 has a temperature dependence that contributes significantly to the overall mechanical qualities of the material. In this report, a method based on flexural frequency response is described in which the variation in the experimental 5^{th} natural frequency under thermal loading is employed to extract the coefficient of thermal dependence of Young's modulus for aluminum 6061-T651. This experimentally obtained coefficient is then employed in the theoretical model to validate the experimental 2^{nd}, 3^{rd}, 4^{th} and 5^{th} natural frequencies of the aluminum beam. A micro-electro-mechanical-systems (MEMS) based microphone sensor is used to monitor the frequency response of the vibrating beam. The theoretical model is based on a *free-free* boundary supported beam from which the natural frequencies are obtained. Constant geometry and constant elasticity models are also presented and compared.

Results

The coefficient of thermal dependence of Young's modulus of elasticity (CTY) for aluminum 6061-T651 obtained by using this approach is in close agreement with published values. It was then employed to obtain the theoretical 2^{nd}, 3^{rd}, 4^{th} and 5^{th} natural frequencies for the aluminum beam. The experimental results obtained herein are in closer agreement with the theoretical model presented in this work employing the experimentally obtained CTY value than with the model using the published CTY value. Modeling also shows that aluminum 6061-T651 has a greater elastic dependence than geometrical to applied thermal loads.

Significance

Aluminum 6061-T651 is widely used in aerospace applications. Accurate material parameters are important when trying to optimize the performance of a given component.

Future plans

To extend these tests to other aerospace aluminum such as 2024 and 7075 and to continue pursuing MEMS based technology for structural health monitoring applications.

This page intentionally left blank.

Sommaire

MEMS Based Acoustic Thermomechanical Characterization of Aluminum 6061-T651 Beams

Rinaldi, G.; DRDC Atlantic TM 2009-080; R & D pour la défense Canada – Atlantique; Septembre 2009.

Introduction ou contexte

Les tests basés sur la température constituent un outil précieux et important pour la détermination des caractéristiques mécaniques de structures. À cet égard, les structures métalliques, comme les poutres en aluminium, répondent aux températures basses ou élevées en se contractant ou en se dilatant. La propriété élastique de l'aluminium 6061-T651 a une dépendance en température qui contribue de manière significative aux qualités mécaniques générales de ce matériau. Dans le cas présent, on décrit une méthode basée sur la réponse en fréquence à la flexion pour laquelle la variation de la $5^{ème}$ fréquence naturelle expérimentale sous charge thermique est utilisée pour extraire le coefficient de dépendance thermique du module d'élasticité de l'aluminium 6061-T651. Ce coefficient expérimental est ensuite utilisé dans le modèle théorique pour valider les $2^{ème}$, $3^{ème}$, $4^{ème}$ et $5^{ème}$ fréquences naturelles expérimentales de la poutre en aluminium. On utilise un microphone basé sur un système micro-électromécanique (SMEM) pour suivre la réponse en fréquence de la poutre vibrante. Le modèle théorique est basé sur une poutre soutenue à limites *libre-libre* à partir de la quelle on obtient les fréquences naturelles. On présente aussi des modèles à élasticité constante et à géométrie constante et on les compare.

Résultats

Le coefficient de dépendance thermique du module d'élasticité obtenu pour l'aluminium 6061-T651 en suivant cette approche est en bon accord avec les valeurs publiées. On l'a ensuite utilisé pour obtenir les $2^{ème}$, $3^{ème}$, $4^{ème}$ et $5^{ème}$ fréquences naturelles théoriques de la poutre en aluminium. Les résultats expérimentaux obtenus concordent mieux à ceux obtenus avec le modèle théorique présenté dans le présent travail en utilisant la valeur du module d'élasticité obtenue expérimentalement qu'avec ceux obtenus avec le modèle en utilisant la valeur publiée du module d'élasticité. La modélisation a aussi montré que l'aluminium 6061-T651 soumis à des charges thermiques a une dépendance élastique plus importante que sa dépendance géométrique.

Importance

L'aluminium 6061-T651 est largement utilisé pour des applications aérospatiales. L'obtention de paramètres précis sur ce matériau est importante quand on essaie d'optimiser la performance d'un composant donné.

Perspectives

Appliquer ces tests à d’autres aluminiums de qualités différentes utilisés en aérospatiale, comme le 2024 et le 7075, et continuer le développement de technologie basée sur les SMEM pour des applications de surveillance de l’état de la structure.

Table of contents

List of figures

List of tables

Acknowledgements

The author would like to thank Mr. Brian Moyes, Mr. Thomas Benak and Mr. Mike Brothers from NRC-IAR, for their help in the experimental setup and for the preparation of the aluminum beams. The author also acknowledges Dr. Ion Stiharu from the Department of Mechanical & Industrial Engineering, Concordia University, Montreal, QC, for his help in developing the MEMS sensor.

This page intentionally left blank.

1. Introduction

1.1 Background

Due to their excellent strength-to-weight ratio aluminum alloys are extensively used in aircraft, automotive and railway structures [1]. In this regard, aluminum 6061 is widely used in the construction of a variety of structures, such as aircraft wings and fuselages and bicycle frames [2]. It is the least expensive and most versatile of the heat-treatable aluminum alloys offering a range of good mechanical properties and good corrosion resistance [3, 4]. The composition of aluminum 6061 alloy by weight % is: silicon minimum 0.4%, maximum 0.8%; iron no minimum, maximum 0.7%; copper minimum 0.15%, maximum 0.40%; manganese no minimum, maximum 0.15%; magnesium minimum 0.8%, maximum 1.2%; chromium minimum 0.04%, maximum 0.35%; zinc no minimum, maximum 0.25%; titanium no minimum, maximum 0.15%; aluminum minimum 95.8%, maximum 98.6%; other elements no more than 0.05% each, 0.15% total [2, 5].

1.2 Heat treatment and temper designations

The mechanical properties of aluminum 6061 depend greatly on the temper, or heat treatment, applied to the material [5-7]. Therefore, in general, materials used in structural applications have to preserve their mechanical characteristics during the service life of the component. While light weight aluminum alloys have excellent corrosion resistance and strength as compared to other structural steels, they have a major drawback in that they lose strength at elevated temperatures [8, 9].

The aluminum industry employs a four-digit (XXXX) index system for the designation of its aluminum alloys [10]. The first digit indicates the alloy group according to the major alloying elements. The second digit indicates modifications in the impurity limits. If the second digit is zero, there is no special control on individual impurities. Digits 1 through 9, which are assigned consecutively as needed, indicate special control of one or more individual impurities. The last two digits indicate specific minimum aluminum content. Although the absolute minimum aluminum content is 99%, the minimum for certain grades is higher than 99%, hence the last two digits are used to represent the hundredths of a per cent over 99%. Hence**,** the designation 1100 indicates minimum aluminum content of 99.00% with individual impurity control, whereas 1030 would denote 99.30% minimum aluminum without special control on individual impurities. Similarly, the designations 1X30 (X = 1…9) indicate the same 99.30% aluminum purity, however with special control on one or more of the added impurities. Given below are several of the main heat treatments applied to aluminum and their associated properties [4, 5, 10].

- 6061-0: Annealed 6061 (6061-0 temper) has maximum tensile strength (minimum force per unit area required to cause a material to break) of no more than 125 MPa, and maximum yield strength (minimum force per unit area required to cause a material to permanently deform) no more than 55 MPa. The material has an elongation (stretch before ultimate failure) of 25-30 %.

- 6061-T4: T4 temper 6061 has an ultimate tensile strength of at least 207 MPa and yield strength of at least 110 MPa. It has elongation of 16%.
- 6061-T6: T6 temper 6061 has an ultimate tensile strength of at least 290 MPa and yield strength of at least 241 MPa. In thicknesses of 6.35 mm or less, it has elongation of 8% or more; in thicker sections, it has elongation of 10%. T651 temper has similar mechanical properties.

Temper designations of wrought aluminum alloys consist of suffixes to the numeric alloy designations [10]. For example, in 6061-T651, 6061 denotes the alloy and T651 refers to the temper applied. The numerical temper designation also indicates the method by which the particular hardness was obtained. For example,

- T6: Solution heat treated and then artificially aged.
- T651: Solution heat treated, stress-relieved by stretching and artificially aged.

1.3 MEMS based sensor

Micro-electro-mechanical-systems (MEMS) technology is an enabling technology that integrates mechanical elements and electronics on a common silicon substrate. MEMS components are currently employed in such diverse areas as cell-biology and DNA analysis to space exploration [11-14]. MEMS technology offers reduced size/weight and low power consumption [15]. Their small size also allows for sensing redundancy within local or global sensing areas, thereby increasing system reliability and safety.

1.3.1 MEMS microphone

Due their high sensitivity, low profile and small footprint, MEMS silicon microphones are proposed as the main components of the sensor [16]. Illustrated in Figure 1 are the principle components of the MEMS based microphone sensor. The sensor consists of two Knowles Acoustics microphones [16] (Figure 1a) bonded onto a miniaturized circuit board (Figure 1b). Two microphones were used for redundancy in the measurements. The entire assembly is then potted within a stainless steel package (Figure 1c). The surrounding epoxy ensures that the microphones are securely fastened within the stainless steel package and can also provide protection against high mechanical vibrations. The relatively large stainless steel package was designed in this way for ease of manipulation (support clamps, etc).

In this work, the proposed acoustic detection approach is based on the well know coin-tap-test [17, 18]. In this approach, a tap is applied manually to the beam for the base excitation in order to generate the natural frequencies of the beam. The MEMS microphone sensor is then used to detect and track the natural frequencies as a function of the applied thermal load.

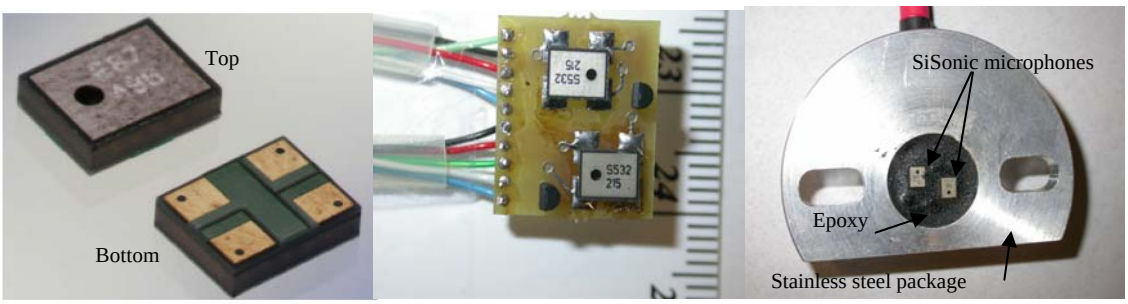

Figure 1: (a) SiSonic microphones. (b) Circuit board layout. (c) Final pressure sensor assembly showing two sensors.

2. Theoretical Model

The nature of the experimental setup, with regard to the boundary support conditions for the aluminum beam, presented herein in the next section requires the dynamic analysis of two models consisting of different boundary support conditions in order to properly compare the results obtained experimentally to the theoretical ones. For all the theoretical analysis the dimensions of beam are the ones of the beam employed in the experimental investigation. They are given in Table 1.

Table 1: Geometrical and elastic parameters for the aluminum beam employed in the theoretical analysis and experimental investigation.

Length (cm)	Width (cm)	Thickness (cm)	Density (kgm^{-3})	Young's Modulus (GPa)
38.99	5.08	0.64	2700	68.9

2.1 Boundary support conditions

The two models presented have *free-free* and *simply supported-simply supported* (here forthwith referred to as *simply-simply*) boundary support conditions, respectively. In both cases the natural frequencies may be estimated from [19],

$$f_i = \frac{\lambda_i}{2\pi}\sqrt{\frac{Eh^2}{12\rho L^4}} \tag{1}$$

where the main difference between the two models are the eigenvalues λ_i obtained for the particular boundary support condition. In Equation (1) f_i are the natural frequencies, E is Young's modulus of elasticity, h is the thickness of the beam, ρ the material density and L the length of the beam.

2.2 Elastic foundation

Shown in Figure 2 is an artificial spring model [20] consisting of translational K_T and rotational K_R springs that can be used to theoretically vary the boundary support conditions for a supported beam structure between *free-free* and *simply-simply* [20]. In this figure, Λ is the positional coordinate along the length of the beam. For *free-free* boundary support conditions $K_T = K_R = 0$, while for *simply-simply* boundary support conditions $K_T = \infty$ and $K_R = 0$. For the condition, $K_T = K_R = \infty$, the beam would have *clamped-clamped* boundary support conditions (not investigated herein).

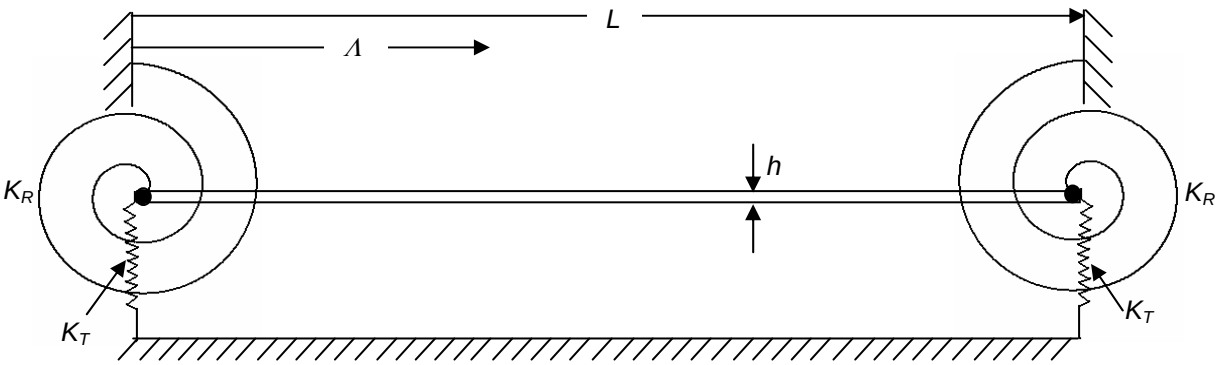

Figure 2: Artificial spring model for varying the boundary support conditions between free-free and simply supported-simply supported.

2.2.1 Natural frequencies and mode shapes

Given in Table 2 is a comparison of the eigenvalues and natural frequencies obtained for *free-free* and *simply-simply* boundary support conditions, respectively.

Table 2: A comparison of the first 5 eigenvalues and associated natural frequencies for a beam with either free-free or simply-simply boundary support conditions.

Flexural Mode	*Free-Free* Eigenvalues	Frequency (Hz)	*Simply-Simply* Eigenvalues	Frequency (Hz)
1	22.4	217	9.87	96
2	61.7	598	39.5	383
3	120.9	1172	88.8	862
4	200	1939	157.9	1532
5	298	2890	246.7	2395

The mode shapes of a vibrating beam, for a given set of boundary conditions, may be obtained from [21],

$$Y(x) = a\sin\lambda_i x + b\sinh\lambda_i x + \alpha_i\left[c\cos\lambda_i x + d\cosh\lambda_i x\right] \tag{2}$$

where $x = \Lambda/L$, and where for *simply-simply* and *free-free* boundary support conditions, respectively,

$$a = 1, b = c = d = \alpha = 0 \tag{2a}$$

$$a = b = 1, c = d = -1, \alpha = \frac{\sinh\lambda_i l - \sin\lambda_i l}{\cosh\lambda_i l - \cos\lambda_i l} \tag{2b}$$

and where,

$$\lambda_i l = \sqrt{eigenvalues} \text{ (as given in Table 1)} \tag{2c}$$

In the experiments presented in the next section, the 5th natural frequency is employed as the reference frequency and is used to extract the mechanical characteristics of the beam in order to obtain the lower frequency vibration modes. However, in order to illustrate the differences in the flexural deflections between *free-free* and *simply-simply* boundary support conditions, the first five mode shapes are compared and presented in Figures 3-7

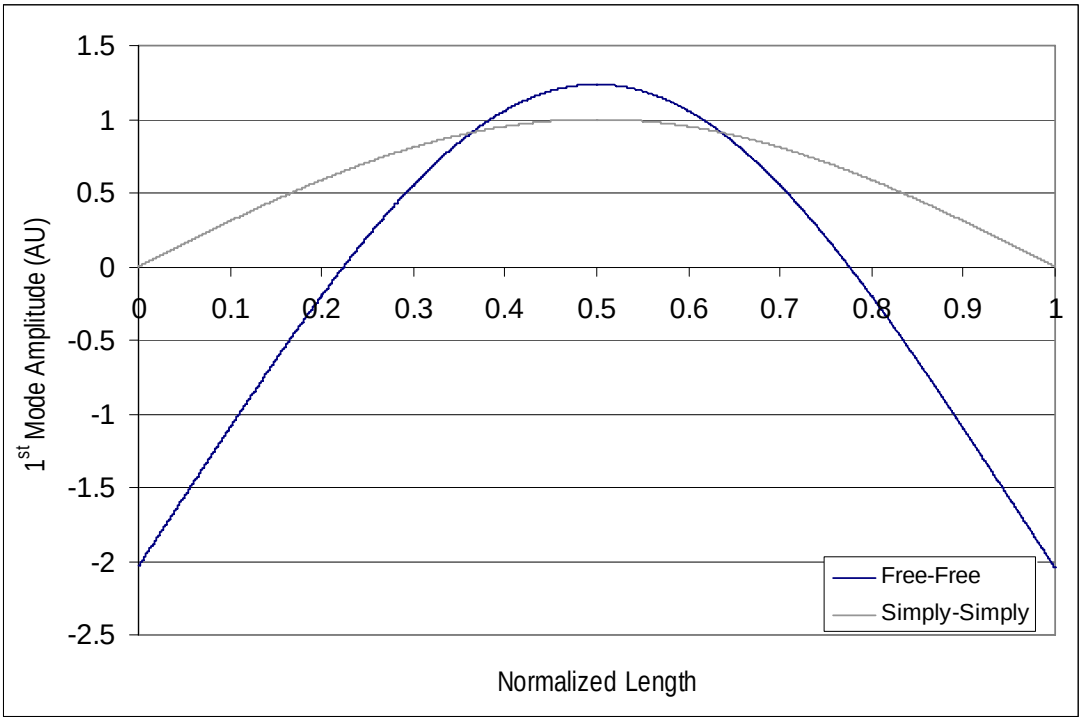

Figure 3: A comparison of the 1st flexural mode deflection for free-free and simply-simply boundary support conditions, respectively.

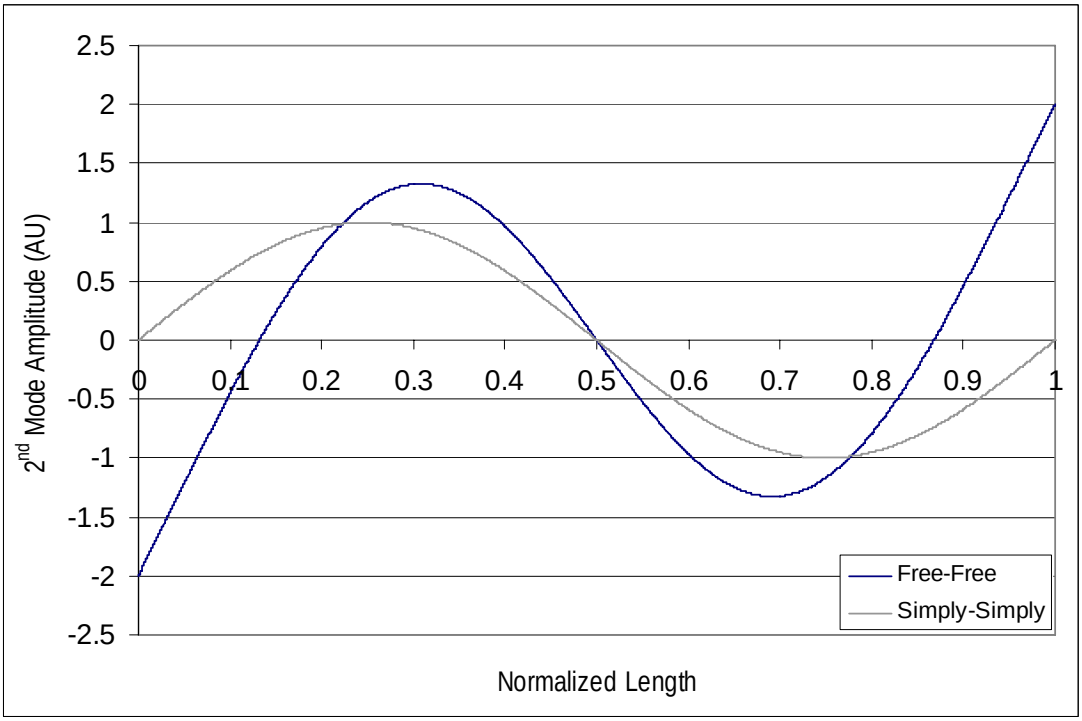

Figure 4: A comparison of the 2nd flexural mode deflection for free-free and simply-simply boundary support conditions, respectively.

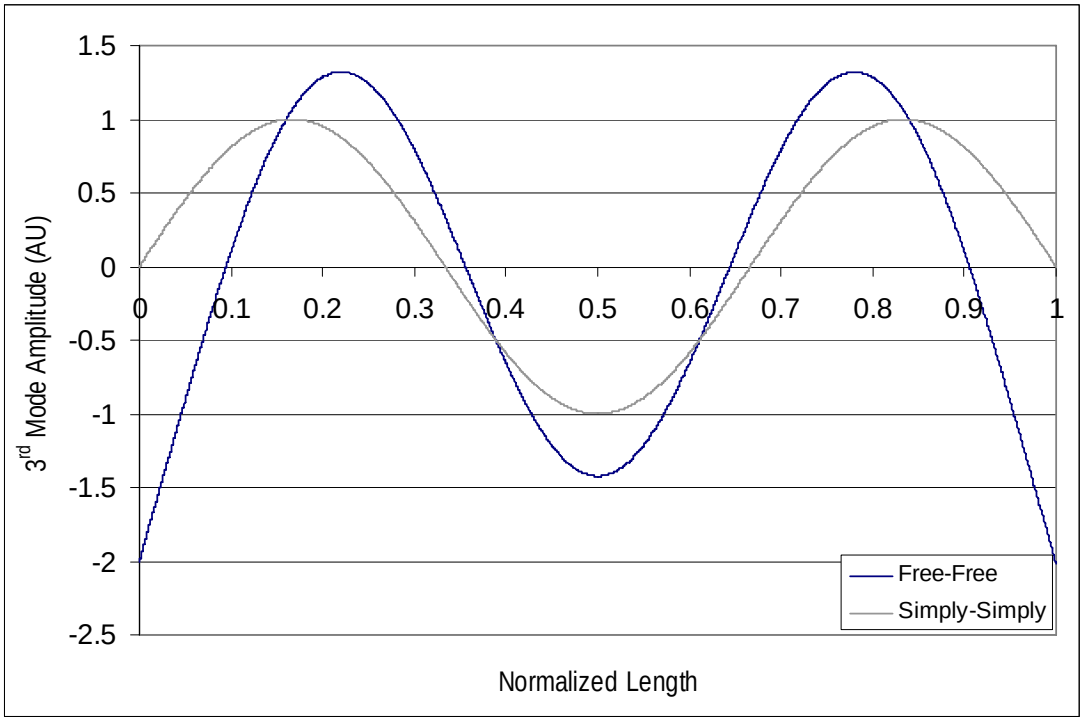

Figure 5: A comparison of the 3rd flexural mode deflection for free-free and simply-simply boundary support conditions, respectively.

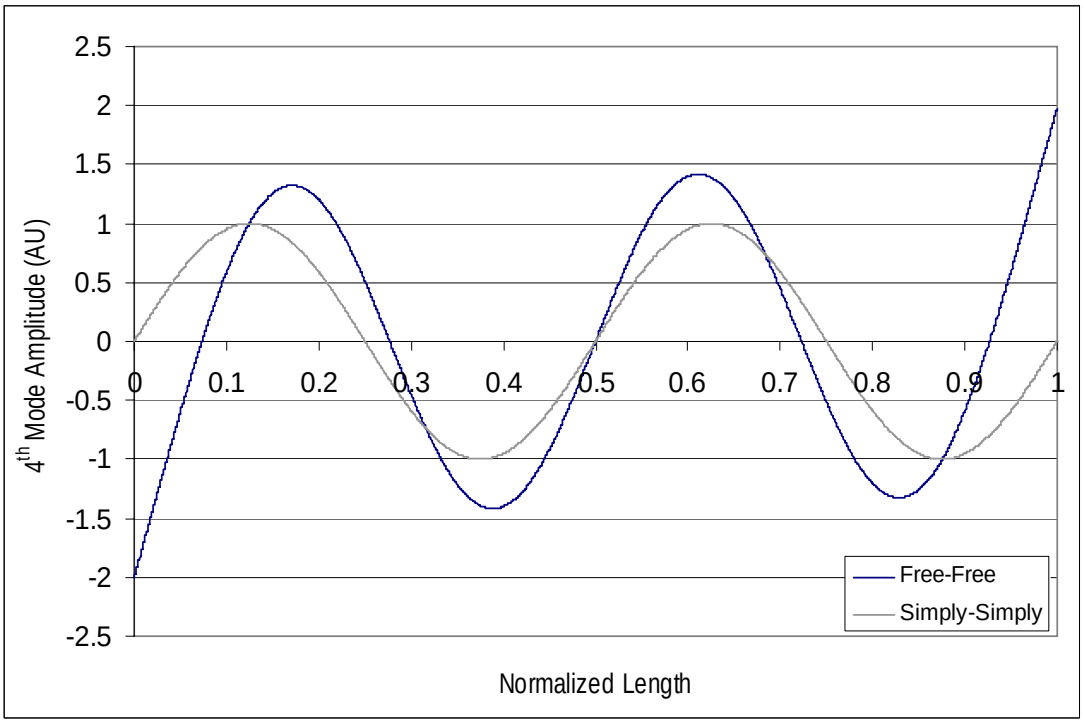

Figure 6: A comparison of the 4th flexural mode deflection for free-free and simply-simply boundary support conditions, respectively.

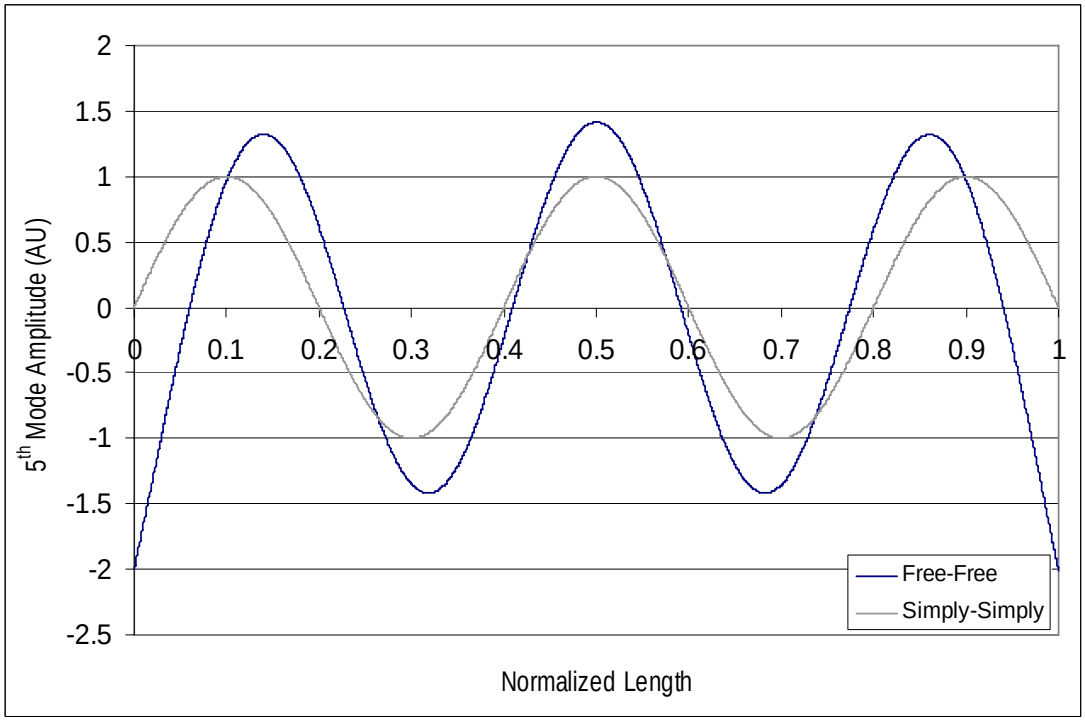

Figure 7: A comparison of the 5th flexural mode deflection for free-free and simply-simply boundary support conditions, respectively.

2.3 Thermal influences

The static and dynamic characteristics of the aluminum beams are tied to the environment to which the beams are exposed. Temperature gradients will influence the mechanical properties of aluminum [22-24]. In this regard, the principal physical quantities affected by temperature include Young's modulus of elasticity and the density (volume) of the material. Hence, when investigating the dynamic properties of aluminum 6061-T651 it is important to incorporate changes to these two physical quantities as a function of the temperature into the model. Also, the thermal dependence of aluminum 6061-T651 on its mechanical characteristics is linear in nature [22], hence the changes in geometry due to the thermal influence can be readily calculated.

2.3.1 Thermomechanical response

The temperature dependence of the natural frequencies can be estimated from the following set of equations [25],

$$f_i(T) = \frac{\lambda_i}{2\pi}\sqrt{\frac{E(T)h^2(T)}{12\rho(T)L^4(T)}} \tag{3}$$

where f_i, E, h, ρ and L are all temperature depended variables. The temperature dependence of each variable is indicated by (T). With respect to Equation (3) the following definitions apply,

$$L(T) = L + \Delta L; \quad \Delta L = L \times CTE \times \Delta T \tag{3a}$$

$$h(T) = h + \Delta h; \quad \Delta h = h \times CTE \times \Delta T \tag{3b}$$

$$w(T) = w + \Delta w; \quad \Delta w = w \times CTE \times \Delta T \tag{3c}$$

where w is the width of the beam and CTE is the coefficient of thermal expansion for 6061-T651 aluminum and Δ denotes the change in that particular parameter at a given temperature. The change in temperature ΔT is calculated using 21^{o}C as the reference temperature,

$$\Delta T = (T - 21)^o\text{C} \tag{4}$$

The CTE value employed in the theoretical calculations is 23.6μm/m-^{o}C [2, 24, 26], and the thermal dependence of the CTE in the temperature range -25^{o}C to 21^{o}C is 0.037142857140μm/m-^{o}C [27]. At temperatures between 21^{o}C-100^{o}C the CTE remains effectively constant [26]. Shown in Figure 8 is the change in the 5th natural frequency as a function of the normalized volume ($V^* = V(T)/V(21\,^o\text{C})$).

The dependence of the volume on temperature will affect the density of the aluminum beam accordingly. This dependence is given by,

$$\rho(T) = \frac{\rho(21) \times L(21) \times w(21) \times h(21)}{L(T) \times w(T) \times h(T)} \tag{5}$$

Illustrated in Figure 9 is the variation of the 5th natural frequency as a function of the change in normalized density ($\rho^* = \rho(T)/\rho(21\,^o\text{C})$)due to thermal effects on the aluminum beam.

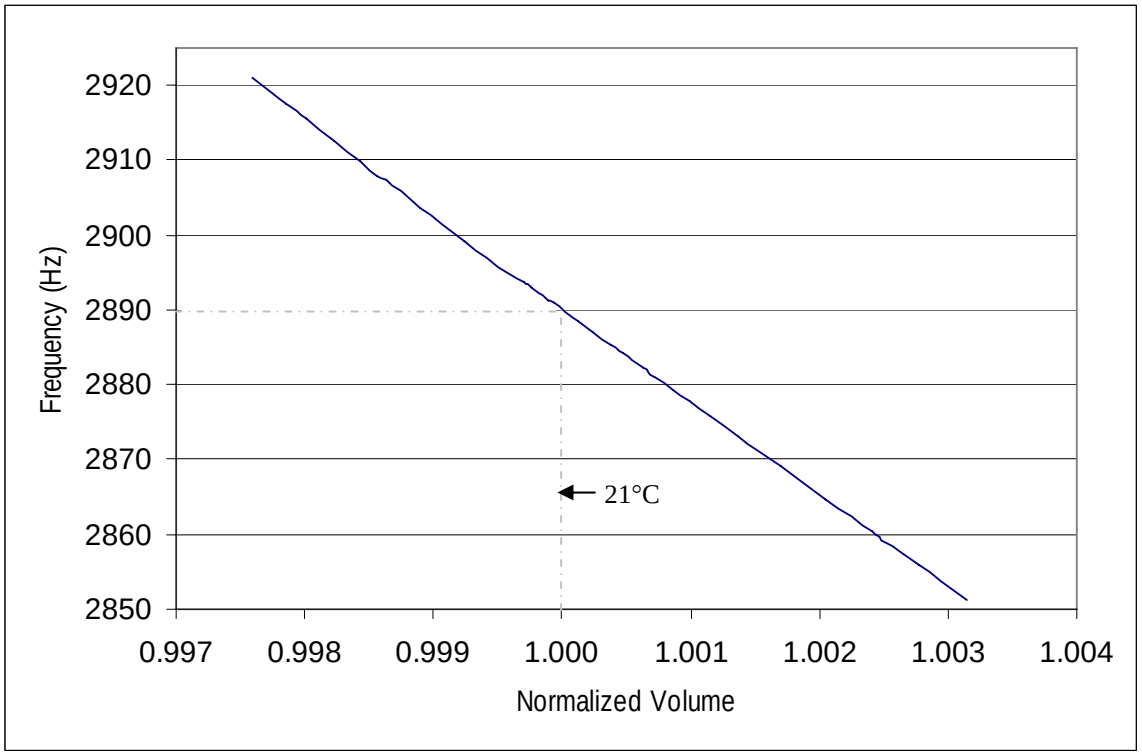

Figure 8: The variation of the natural frequency as a function of the thermally dependent volume.

2.3.1.1 Elasticity thermal dependency

The elasticity, or stiffness of the beam, is also temperature sensitive, hence the change in Young's modulus of elasticity is obtained from,

$$E(T) = E + \Delta E; \quad \Delta E = E \times CTY \times \Delta T \tag{6}$$

where *CTY* is the coefficient of thermal dependence for Young's modulus. The value of -45 MPa/ ^{o}C is found in published works [24, 28], and is employed here in the theoretical model for the 5th natural frequency. Given in Figure 10 is the effect on the 5th natural frequency of the variation in normalized Young's modulus ($E^* = E(T)/E(21\ ^{o}C)$)of elasticity.

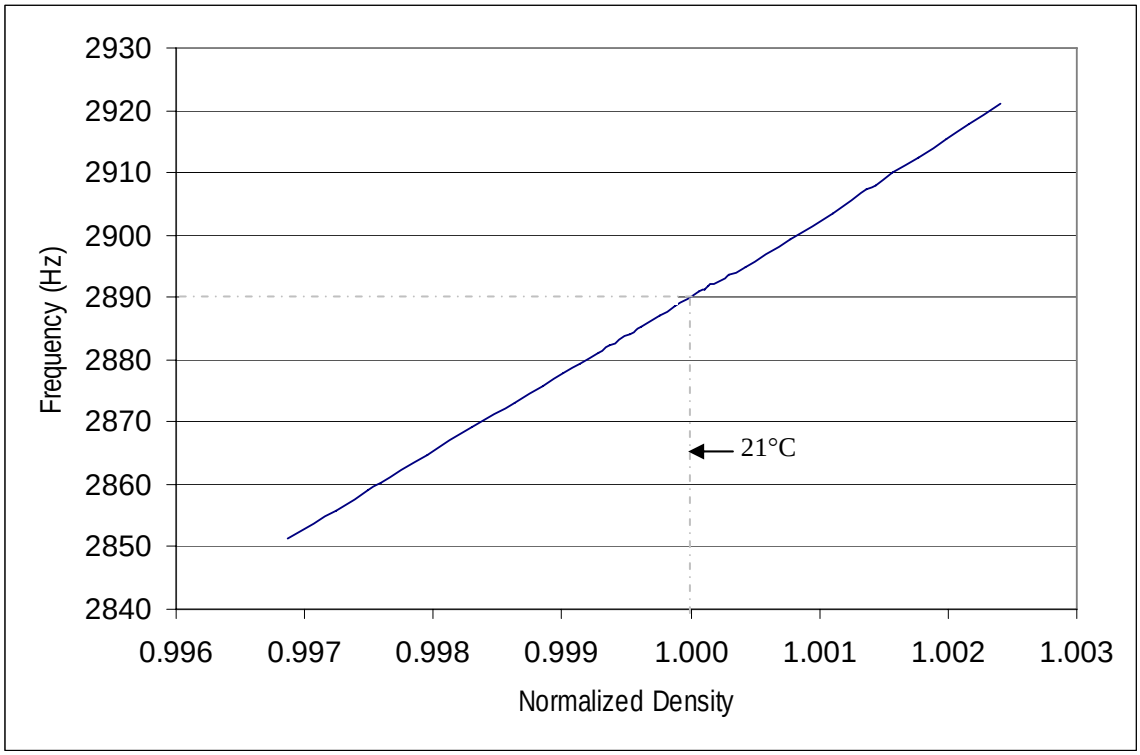

Figure 9: The effect of thermally dependent density on the natural frequency of the aluminum beam.

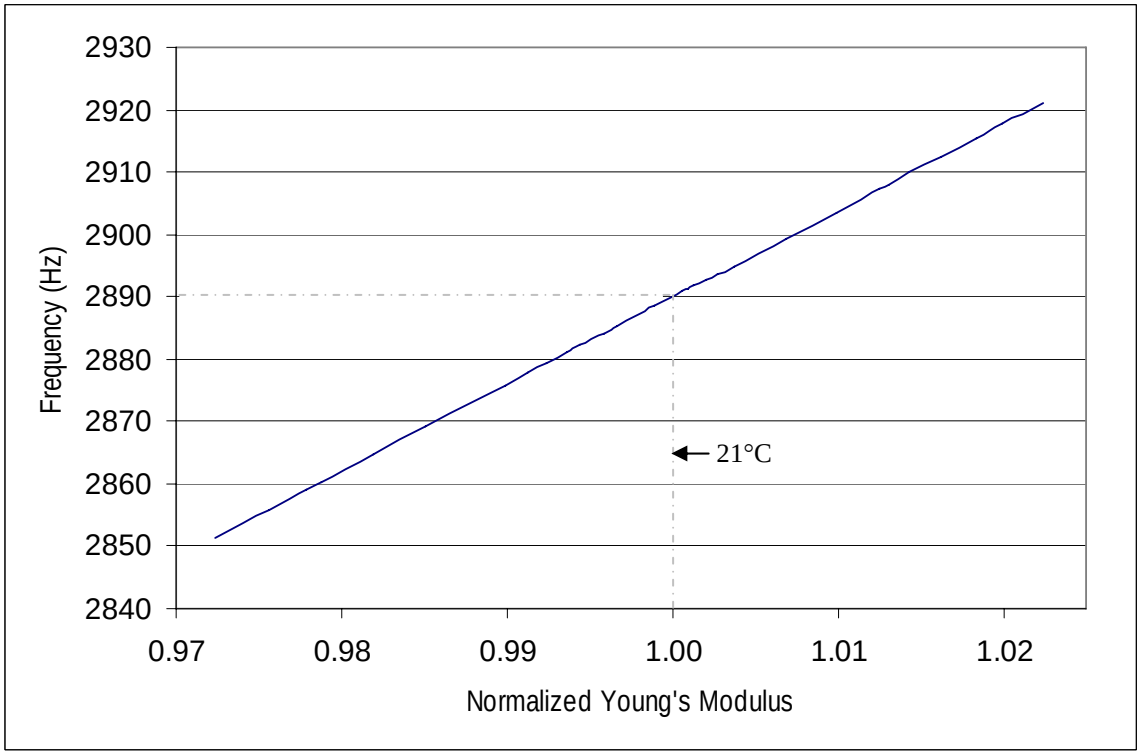

Figure 10: The variation of the natural frequency as a function of the change in Young's modulus.

A direct comparison of the variation in volume, density and Young's modulus as a function of temperature is given in Figure 11. Of these three parameters it can be seen that Young's modulus of elasticity is most readily affected by thermal influences. Given in Table 3 is a comparison of the slopes obtained for the plots in Figs. 8-10.

Table 3: A comparison of the slopes of the curves presented in Figures 8-10.

Parameter (Normalized)	Thermal dependence	Frequency dependence
Volume	6.90×10^{-5} V^*/°C	-12.6kHz/V^*
Density	-6.90×10^{-5} ρ^*/°C	12.6kHz/ρ^*
Young's modulus	-6.23×10^{-4} E^*/°C	1.39kHz/E^*

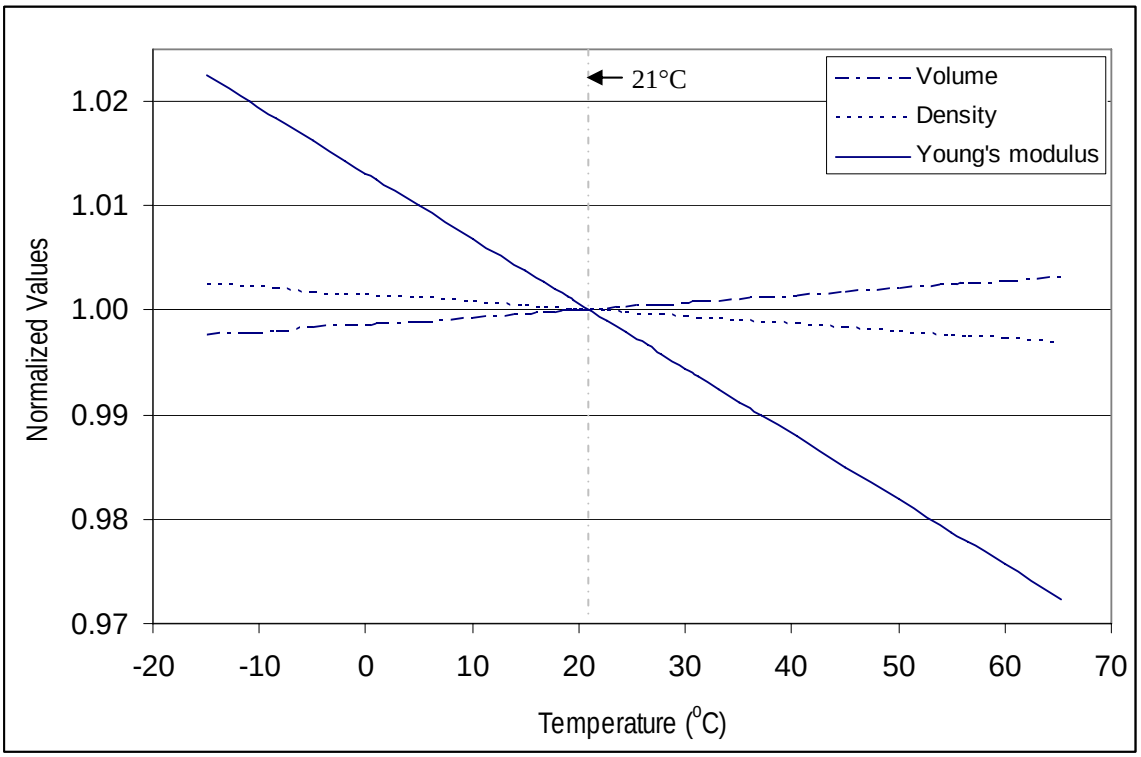

Figure 11: The changes in normalized volume, density and young's modulus as a function of temperature.

The normalized volume V^* increases and decreases with increase and decrease, respectively, in temperature, whereas both the normalized density ρ^* and Young's modulus E^* go against this trend. The variation trends for the normalized values V^*, ρ^* and E^* for the temperature ranges T < 21°C, T = 21°C and T > 21°C are summarized in Table 4.

Table 4: Characterizing the normalized volume, density and Young's modulus as a function of the temperature range.

Normalized Volume	Normalized Density	Normalized Young's Modulus
$V^* < 1; T < 21^\circ\mathrm{C}$	$\rho^* > 1; T < 21^\circ\mathrm{C}$	$E^* > 1; T < 21^\circ\mathrm{C}$
$V^* = 1; T = 21^\circ\mathrm{C}$	$\rho^* = 1; T = 21^\circ\mathrm{C}$	$E^* = 1; T = 21^\circ\mathrm{C}$
$V^* > 1; T > 21^\circ\mathrm{C}$	$\rho^* < 1; T > 21^\circ\mathrm{C}$	$E^* < 1; T > 21^\circ\mathrm{C}$

Shown in Figure 12 is the variation in the 5th natural frequency for each of the normalized parameters.

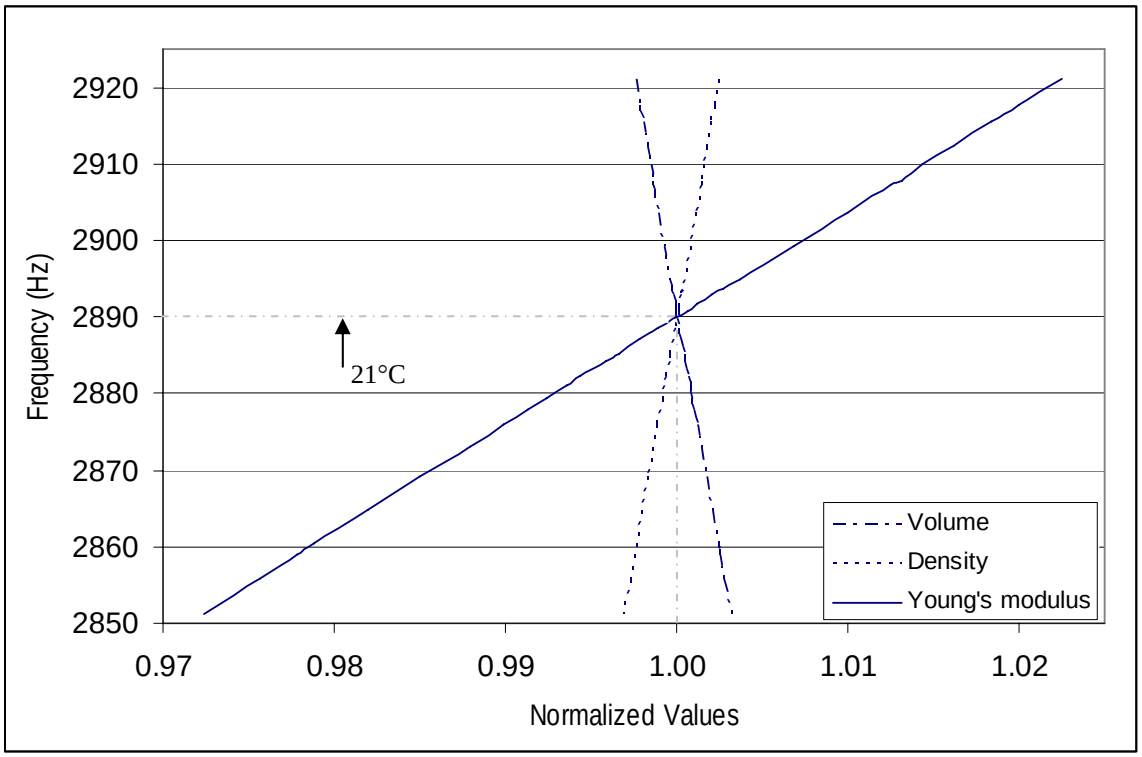

Figure 12: A comparison of the variation in frequency as a function of the normalized physical values.

For aluminum 6061-T651 there is a much greater dependence on temperature for Young's modulus. The slope obtained from Figure 11 for the thermal dependence of Young's modulus is an order of magnitude greater than for the change in density or the change in volume. Hence, when characterizing the influence of temperature on the elastic properties of aluminum the variations to, and due to, Young's modulus must be carefully monitored.

2.4 Prediction of parameters

As the results obtained are linear in nature it is of interest to analyze the results presented in Figures 11-12 further in order to extract more pertinent information regarding the combined influences on the natural frequencies obtained. In this regard, it would be of interest to be able to predict, *a priori*, the changes to these physical quantities based on coupled parameters such as, in the work presented herein, resonance frequency and temperature. Due to the linearity of the variations the parameters may be put into a matrix formulation of the form [29],

$$Ay = B \tag{7}$$

where A is the *influence* matrix consisting of experimentally obtained values, y are the unknown coefficients and B the normalized volume, density and Young's modulus values matrix. In this regard, solving Equation (6) for the coefficient matrix,

$$y = A^{-1}B \tag{7a}$$

would allow for the prediction of the changes to volume, density and Young's modulus at any given temperature, based on resonance measurements, within the temperature range of the experiments presented herein (-15 to 65.3°C). Given in Figure 13 is the 6 x 6 *influence* matrix containing temperature and resonance frequency values, the unknown coefficient matrix $y_1 \ldots y_6$ and the normalized results matrix. Application of Equation (7a) yields the unknown coefficients $y_1 \ldots y_6$.

$$\begin{bmatrix} -15 & 2921.1 & 0 & 0 & 0 & 0 \\ 65.3 & 2851.26 & 0 & 0 & 0 & 0 \\ 0 & 0 & -15 & 2921.1 & 0 & 0 \\ 0 & 0 & 65.3 & 2851.26 & 0 & 0 \\ 0 & 0 & 0 & 0 & -15 & 2921.1 \\ 0 & 0 & 0 & 0 & 65.3 & 2851.26 \end{bmatrix} \begin{bmatrix} y_1 \\ y_2 \\ y_3 \\ y_4 \\ y_5 \\ y_6 \end{bmatrix} = \begin{bmatrix} 0.997598 \\ 1.003139 \\ 1.002408 \\ 0.996870 \\ 1.022460 \\ 0.972362 \end{bmatrix} \begin{matrix} \} \text{Normalized Volume} \\ \\ \} \text{Normalized Density} \\ \\ \} \text{Normalized Young's Modulus} \end{matrix}$$

$$\begin{bmatrix} y_1 = 3.677 & y_2 = 3.434 & y_3 = 2.305 & y_4 = 3.443 & y_5 = -3.209 & y_6 = 3.484 \end{bmatrix} 1 \times 10^{-4}$$

Figure 13: An example of using a matrix formulation to obtain the unknown coefficients $y_1 \ldots y_6$.

2.5 Constant geometry and constant elasticity models

An approach is now presented in which the temperature effects on the geometry and elasticity of the aluminum beam are *discretized* according to that particular domain. In this regard, the constant geometry and constant elasticity models are given by, respectively,

$$f_i(T)_G = \frac{\lambda_i}{2\pi}\sqrt{\frac{E(T)h^2}{12\rho L^4}} \tag{8}$$

$$f_i(T)_K = \frac{\lambda_i}{2\pi}\sqrt{\frac{Eh^2(T)}{12\rho(T)L^4(T)}} \tag{9}$$

where the subscripts *G* and *K* refer to geometry (mass) and elasticity (stiffness), respectively. In this approach it will be possible to determine the dominant influence on the natural frequency of the beam by systematically maintaining either the geometry or elasticity at a constant value and letting the other parameter vary with temperature. Shown in Figure 14 is a comparison of the variation in natural frequency as a function of temperature for the theoretical, constant geometry and constant elasticity models. In this figure, the theoretical curve is obtained from Equation (3). Given in Figure 15 is a comparison of the percent deviation ($(a_1-a_2)/a_1*100\%$) between the theoretical and constant geometry and constant elasticity models, respectively.

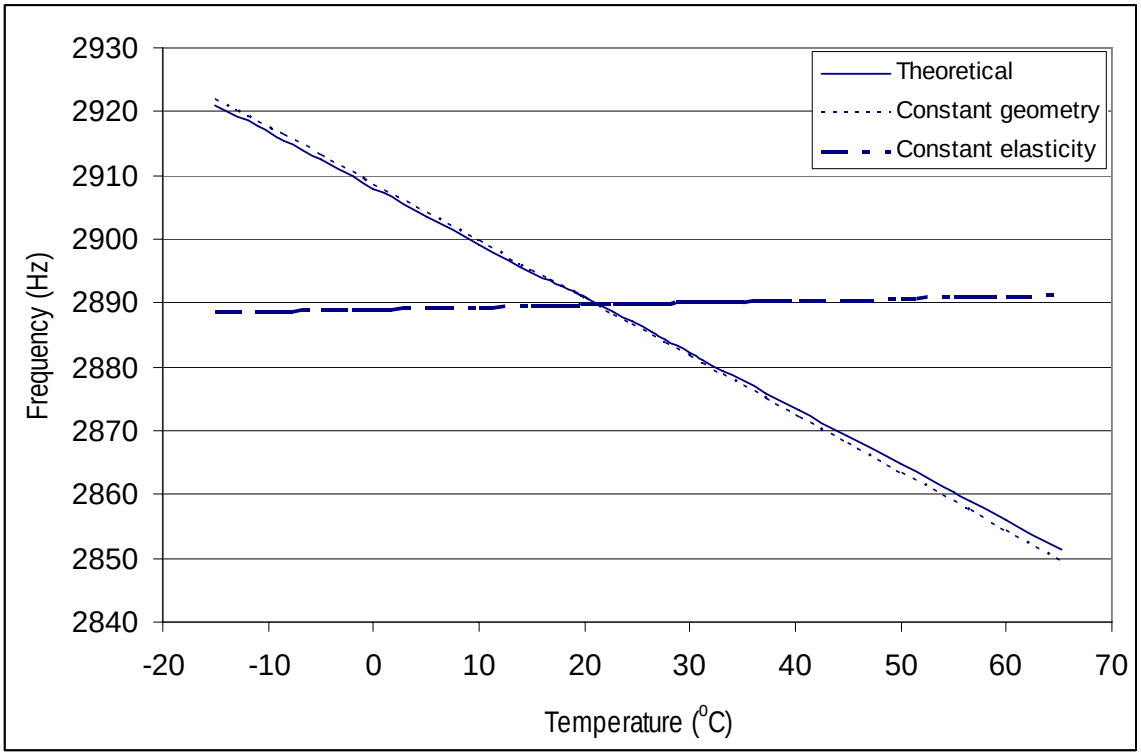

Figure 14: A comparison of the 5th natural frequencies obtained for the theoretical, constant geometry and constant elasticity models.

From Figure 14 it can be seen that the changes in the 5th natural frequency due to the thermal dependence of the geometry are much less than the thermal dependence of the elasticity. The curve for the constant geometry is very close to the actual theoretical values with all temperature dependent parameters. From Figure 15 the predominant dependence of Young's modulus of

elasticity, as compared to the geometry, to thermal influences is clearly seen. An interpretation of these results, given in Table 5, suggest that the slopes (absolute values) obtained for the constant elasticity curve are very close with a slightly higher slope in the range >21°C. However, for the constant geometry curve the slopes vary significantly, with a substantially greater thermal dependence of Young's modulus for aluminum 6061-T651 in the temperature range >21°C.

Table 5: Analysis of the slopes obtained for the curves given in Figure 15.

Temperature range (°C)	Slope of constant geometry plot	Slope of constant elasticity plot
-15→21	-0.00083	-0.03096
21→65.3	0.001411	0.03162
Percent deviation	41.2%	2.1%

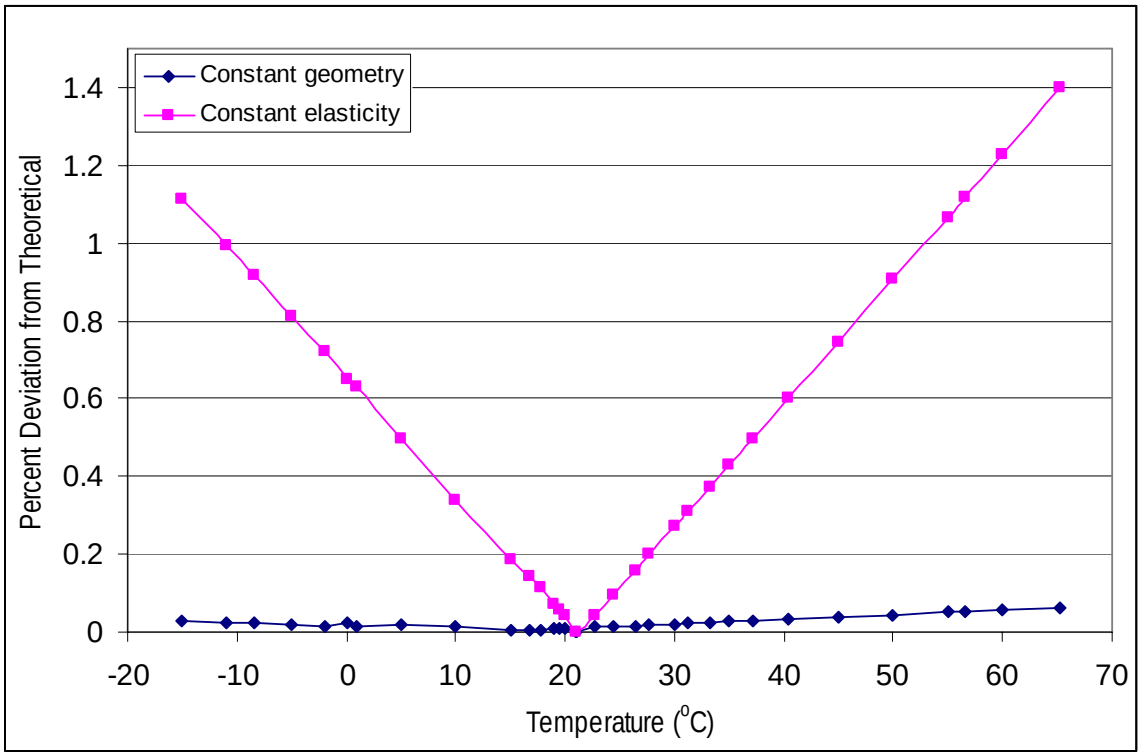

Figure 15: A plot of the absolute percent deviation from the theoretical values shown in Figure 10 for the constant geometry and constant elasticity models.

3. Experimental Section

The main objective of the experiments carried out herein is to predict the theoretical 2nd, 3rd and 4th natural frequencies of an aluminum 6061-T651 beam based on the thermomechanical characteristics obtained from the 5th natural frequency. In employing this approach, the experimental 5th natural frequency is used to augment the theoretical model, particularly the *CTY* value for aluminum 6061-T651, which is then incorporated into the theoretical model to predict the lower frequencies.

3.1 Base excitation

The aluminum 6061-T651 beam was placed onto foam supports. Due to the characteristics of the foam it was not clear, initially, whether the frequency response of the beam would be dominated by *free-free* or *simply-simply* boundary support conditions as discussed above. Shown in Figure 16 is a schematic of the experimental set up employed for the base excitation. A modal impact hammer (Endevco, Model 2302-100) was employed for the base excitation of the aluminum beam. A MEMS based microphone (Knowles Acoustics, Model SiSonic SPM0102ND3) sensor was employed to measure and obtain the resonance frequencies of the beam. An oscilloscope (Tektronix, Model TDS 5104) in FFT mode was used to acquire and analyze the sensor data. Preliminary testing and adjustments of the experimental set up and subsequent initial testing of the frequency response of the aluminum beam revealed that the foam based support boundary conditions were *free-free* in nature as opposed to *simply-simply*.

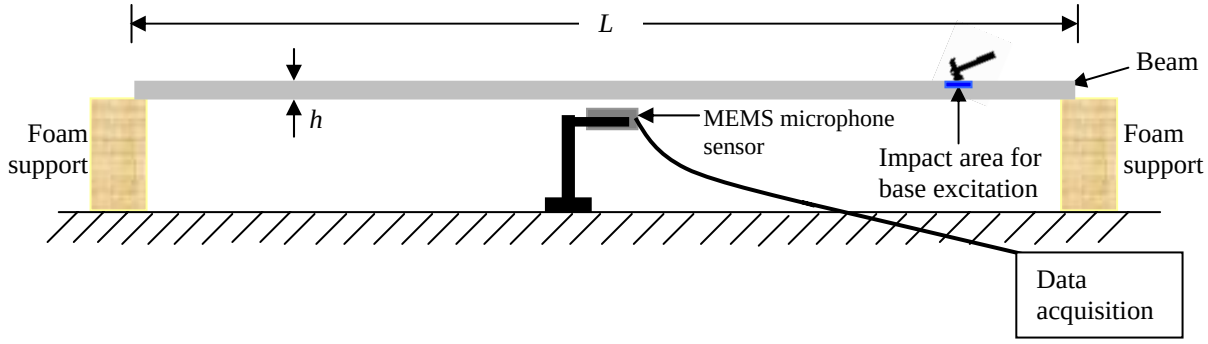

Figure 16: A schematic side-view of the aluminum 6061-T651 beam indicating the placement of the MEMS based sensor and base excitation impact location.

A sample of a typical frequency response obtained using the MEMS microphone is shown in Figure 17.

3.2 Thermal loading

In the experiments carried out herein, the temperature ranged between -15°C to 65.3°C. For the hot temperature measurements, the beam was heat-soaked in an oven (VWR Scientific Instruments Oven, Model 1680) and the resonance measurements were taken every ~5°C decrease until the beam reached room temperature. Similarly, for the cold temperature measurements, the beam was placed into a conventional freezer and allowed to soak for several hours. Resonance measurements were then taken for every ~5°C increase until the beam reached room temperature. The surface temperature of the beam was measured and monitored using a thermometer (Omega, Model HH21 Microprocessor Thermometer) and thermo-couple (Omega, Type K) that was attached with an adhesive strip to the surface of the beam. For these tests, a MEMS microphone was employed to acquire the acoustic signal from the surface of the aluminum beam after an applied tap. Shown in Figure 18 is an overview of the components used in experimentation carried out herein. A supply voltage of ~2VDC was used for powering the microphone. The final experimental set up is presented in Figure 19.

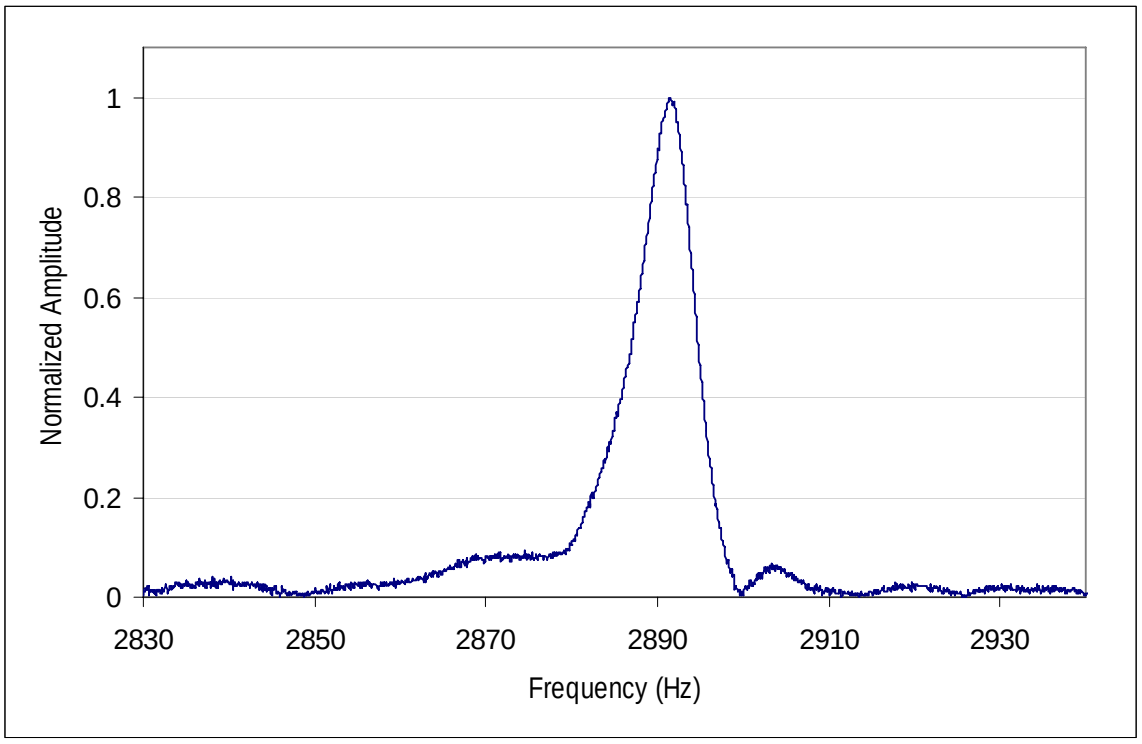

Figure 17: A sample of the 5th natural frequency response obtained employing the experimental set up described herein.

During the course of the preliminary testing it was found that the impact location influenced the number and the amplitude of the resonance modes obtained. In this regard, the consistent acquisition of the 1st resonance mode at the various temperatures proved most difficult. Hence,

the experimental investigation and analysis for the 1st mode was dropped from the work presented herein.

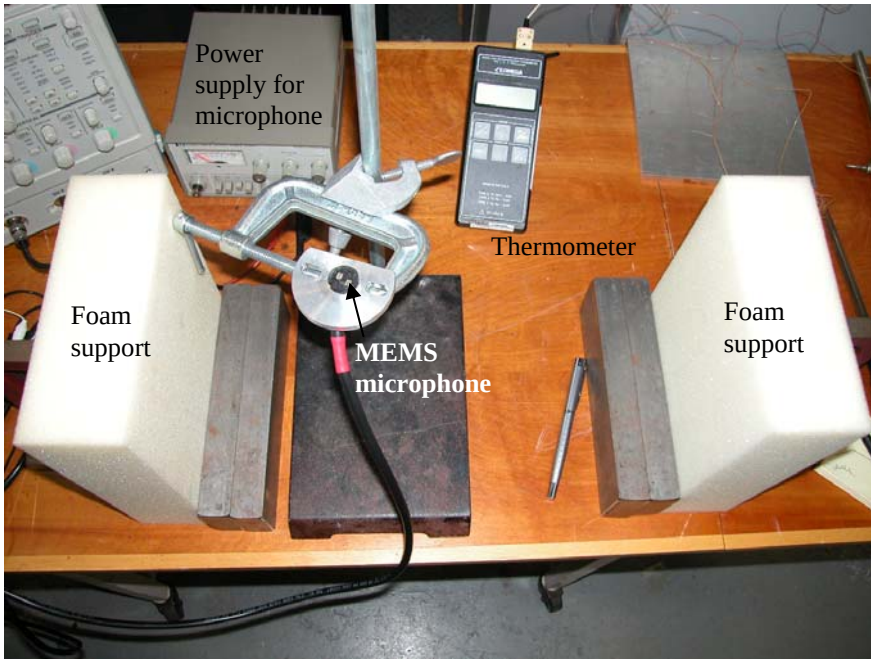

Figure 18: An overview of the experimental setup used for the temperature measurements.

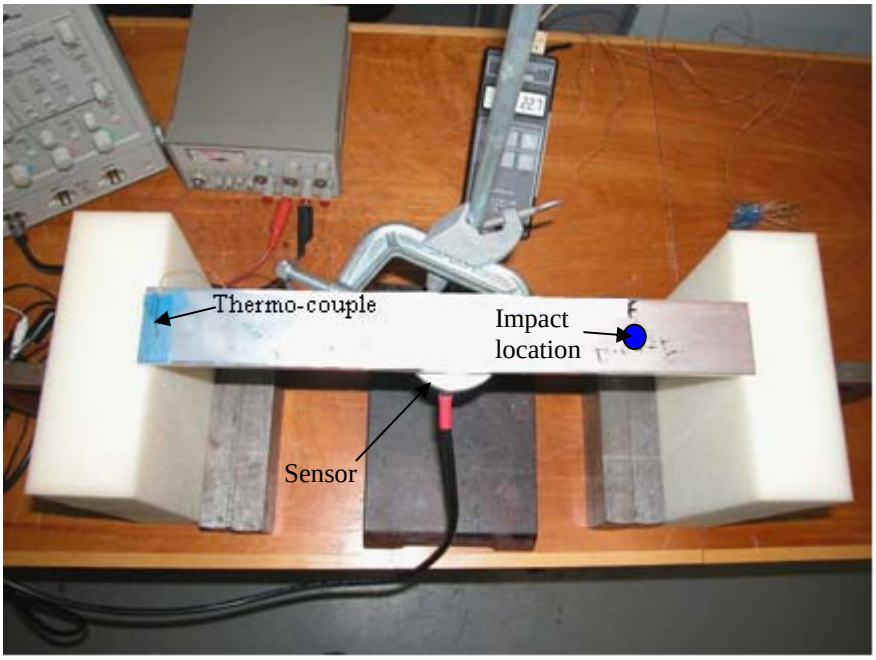

Figure 19: The final positioning of the aluminum beam on the foam supports with the sensor beneath it. The placement of the thermo-couple is also shown.

4. Results and Discussion

The experiments consisted, firstly, of the acquisition of the 5th resonance mode in temperature intervals of ~5°C in the temperature range -15 to 65.3°C. Shown in Figure 20 is the shift in the 5th resonance frequency as a function of temperature (2890 Hz corresponds to 21°C).

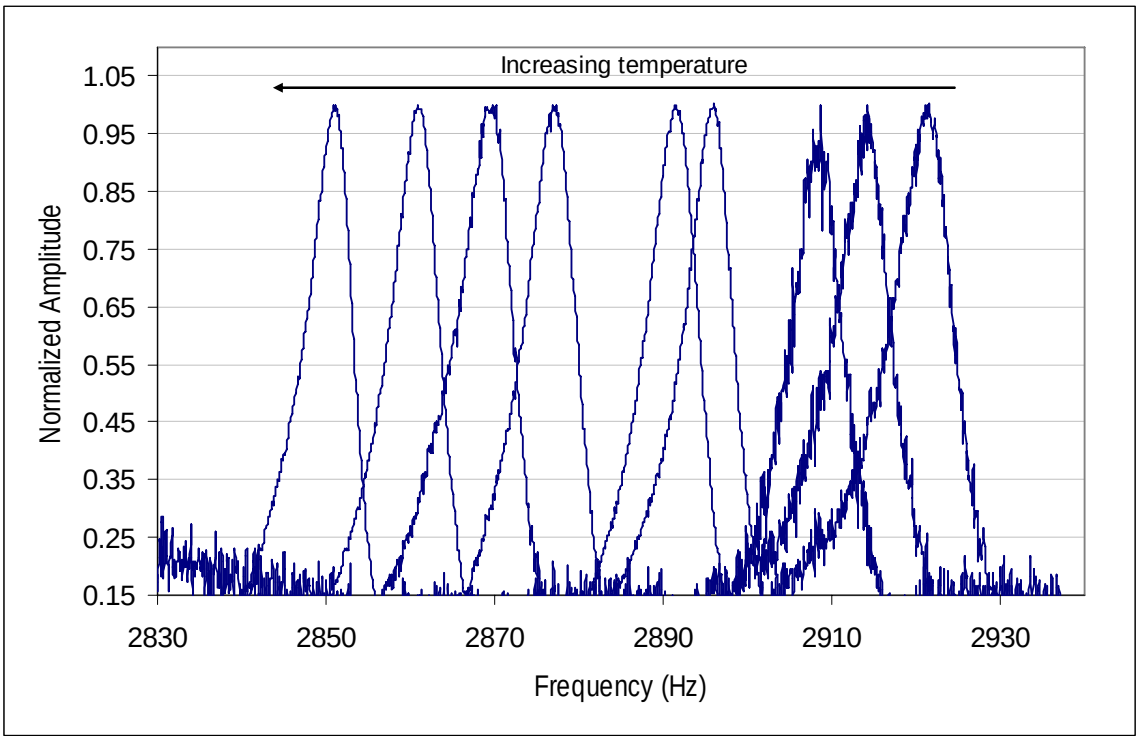

Figure 20: The shift to lower frequency of the 5th natural frequency as a function of increasing temperature.

For the thermal dependence of Young's modulus, the coefficient (*CTY*) value of -42.985714 MPa/°C was determined experimentally (here forthwith referred to as *CTY* experimental) and is consistent with the published value of -45 MPa/°C (here forthwith referred to as *CTY* literature) [23]. This value was obtained by plotting the center frequency of the natural frequency response bandwidth obtained at -15 and 65.3°C. The extremities of the temperature range were used in this regard because it was believed that the thermo-couple and the adhesive employed (Airtech, Flashbreaker 1) would be in good contact with the surface of the aluminum beam as shown in Figure 19. These two experimental end points were then fit with a theoretical curve obtained with a *CTY* value of -42.985714 MPa/°C and Equation (3). This is shown in Figure 21. Given in Table 6 are the equations for the curves given in Figure 17.

Table 6: The equations used to generate the fitted curves for the beam investigated.

CTY (MPa/°C)	Equation
-45	-0.9119T + 2908.6
-42.985714	-08696T + 2908.1

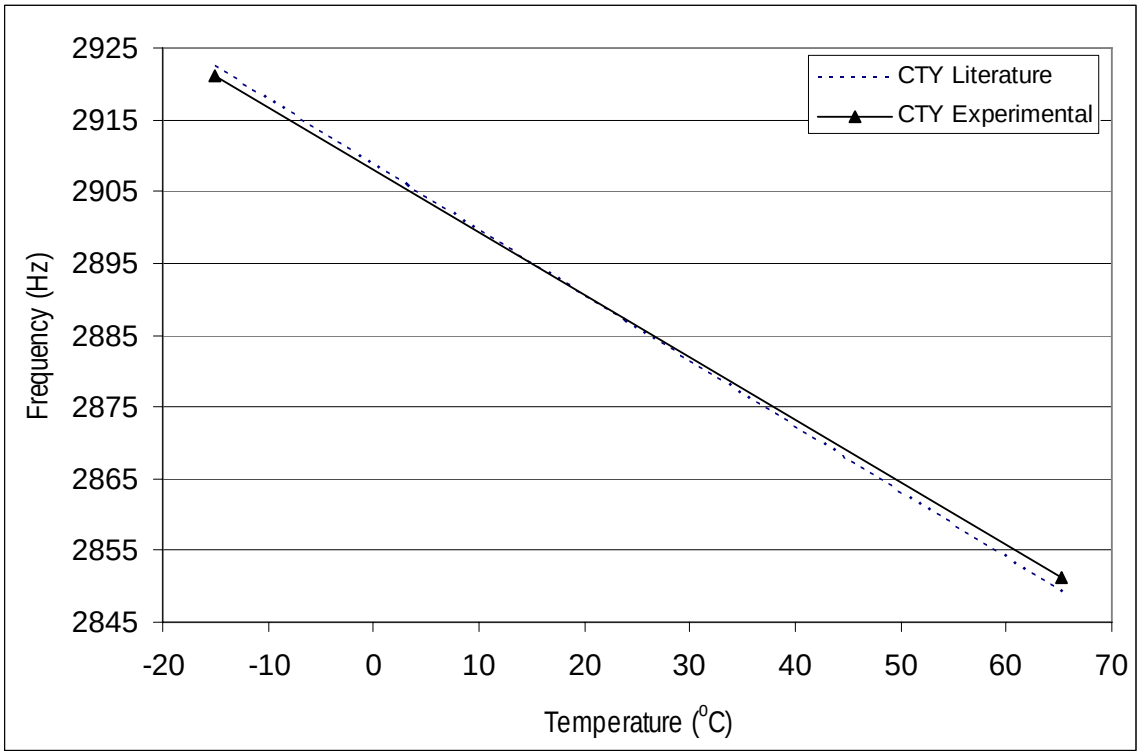

Figure 21: A comparison of the coefficients of thermal dependence for Young's modulus (CTY) found in the literature and the experimentally obtained value.

The center frequencies obtained as a function of temperature were then plotted to determine if they would follow the trend of the experimental *CTY* curve as shown in Figure 21. This is shown in Figure 22. In this figure, the effects of the adhesive disbonding from the aluminum surface can be seen in part through the deviation of the experimental results from both the literature and experimental *CTY* curves. The adhesive disbond would result in an inaccurate temperature measurement from the surface of the aluminum beam due to the thermo-couple's *loss* of contact with the surface. Effects due to condensation on the surface of aluminum beam can also be seen. In this regard, the water droplets forming on the beam increased its mass thereby lowering the natural frequency of the beam at that particular temperature.

For the measurements for the 2nd, 3rd and 4th natural frequencies, the impact location on the aluminum beam was optimized to excite that particular mode (high amplitude response). Hence, for the 2nd, 3rd and 4th modes, respectively, the impact locations were $x \approx 0.3$, $x \approx 0.5$ and $x \approx 0.4$.

In order to avoid the concerns regarding condensation effects, cold temperature measurements were not taken for these tests. Also, the bandwidth on the oscilloscope was limited to that particular frequency response ± 100 Hz about the center frequency for each frequency response investigated. In each case the experimentally determined *CTY* value was used for the theoretical analysis. Shown in Figures 23-25 are the experimental and theoretical (*CTY* = -42.985714 MPa/°C) results obtained for the 2nd, 3rd and 4th natural frequencies, respectively, as a function of temperature.

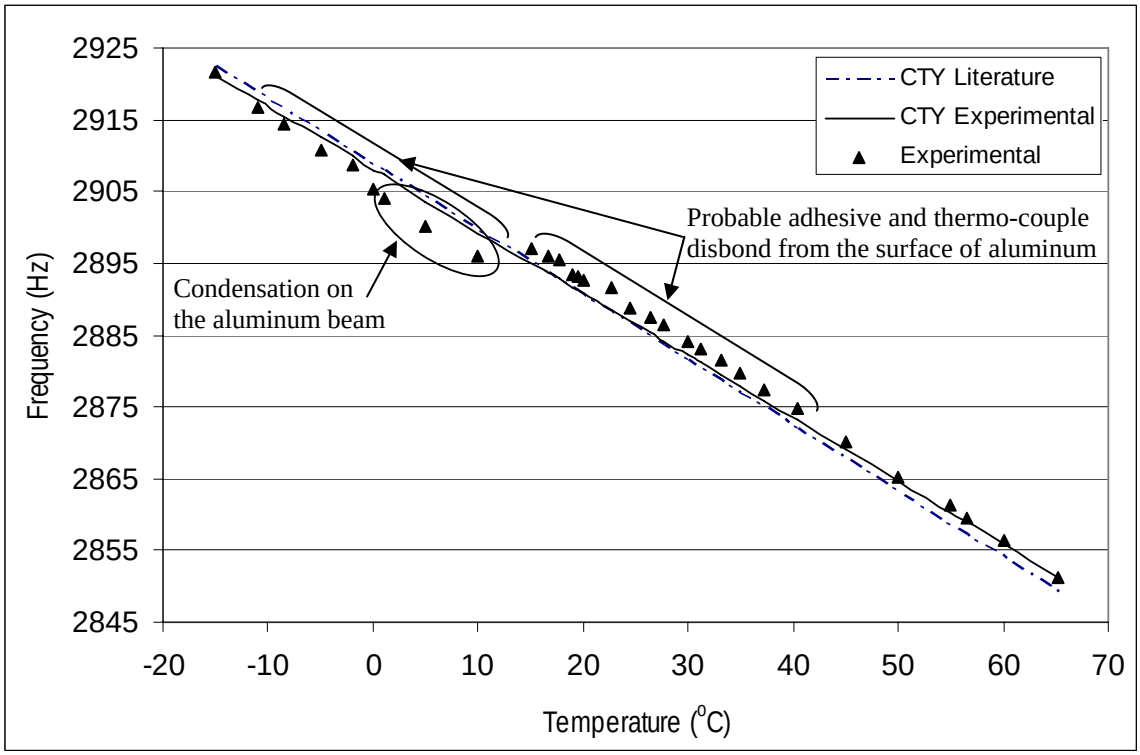

Figure 22: Changes in the 5th resonance frequency as a function of temperature. Experimental and theoretical results are compared. Highlighted areas indicate adhesive and thermo-couple disbond from the aluminum surface. Condensation effects are also indicated.

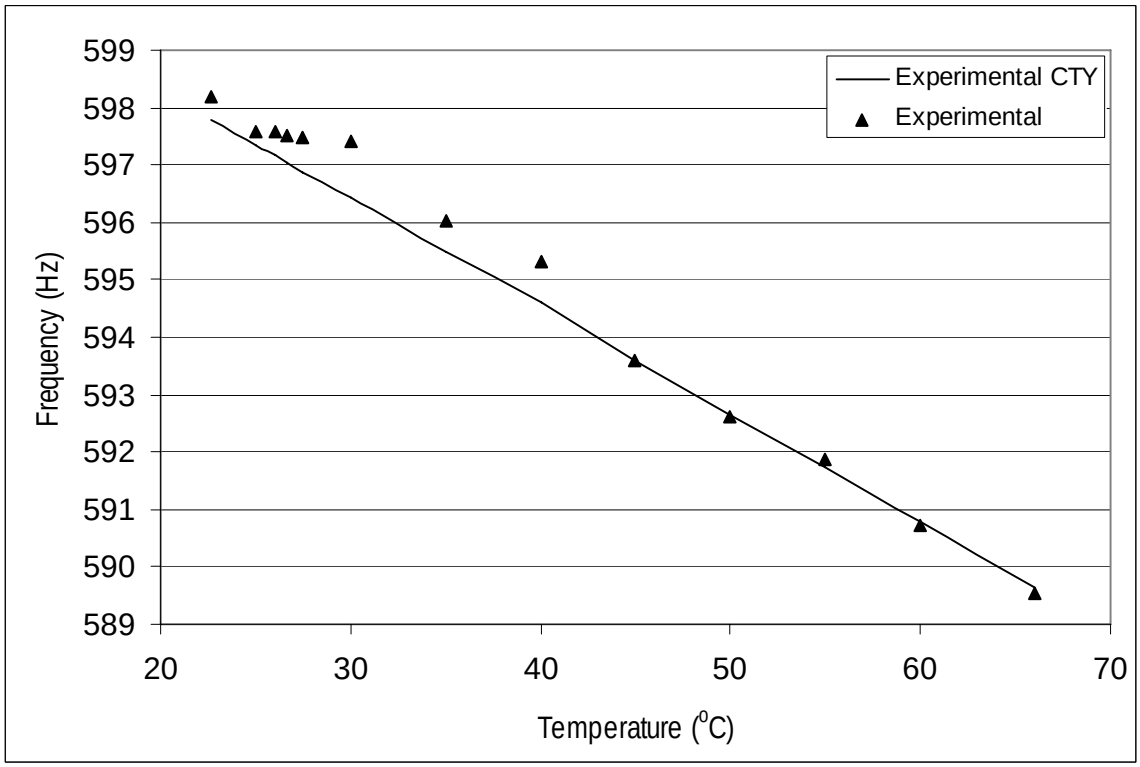

Figure 23: The variation of the 2nd natural frequency as a function of temperature.

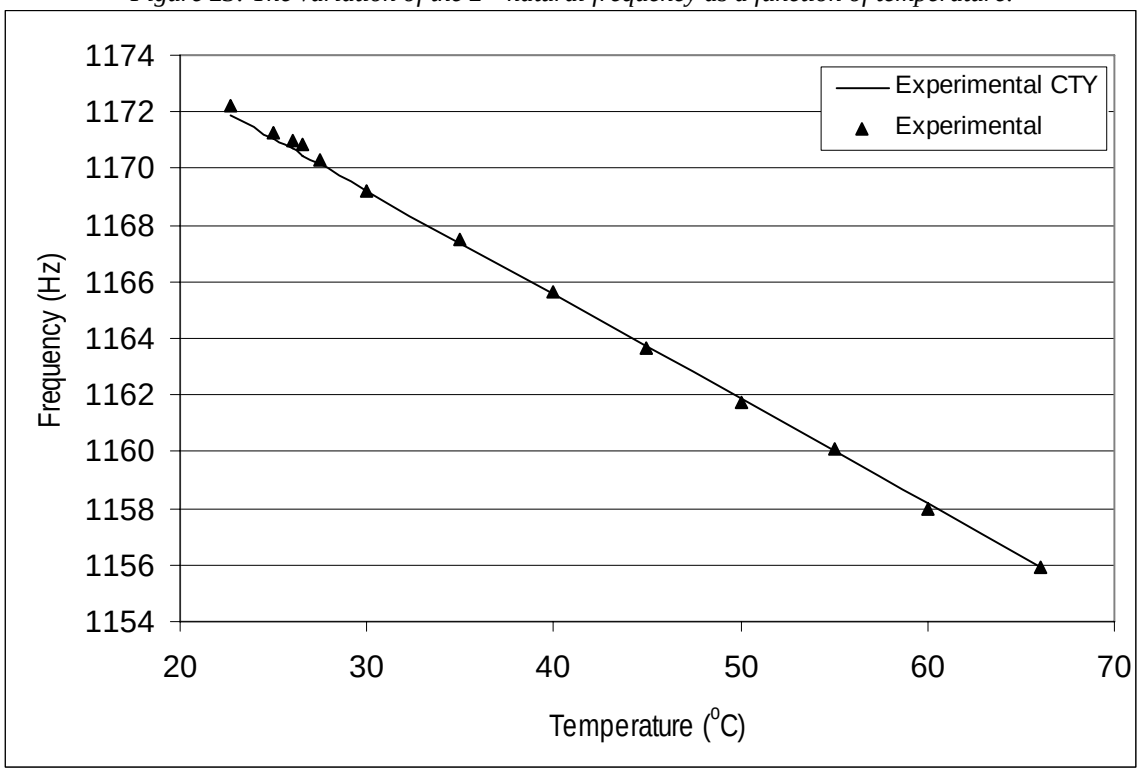

Figure 24: The variation of the 3rd natural frequency as a function of temperature.

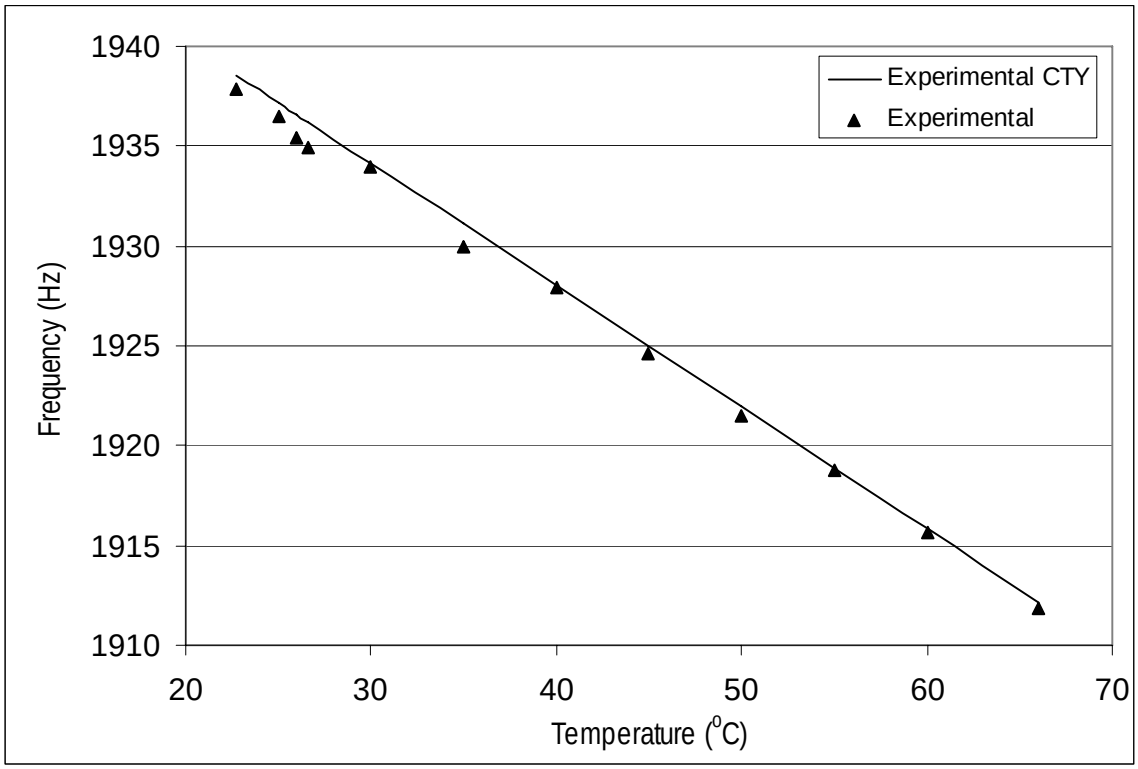

Figure 25: The variation of the 4th natural frequency as a function of temperature.

The results presented above in Figs. 23-25 show a good agreement between the experimental results and the theoretical values obtained employing the *CTY* value of -42.985714 MPa/°C that was determined using the 5th natural frequency. The combined effects of adhesive and thermo-couple disbonds (author's hypothesis for disagreements between theory and experiment) are also visible in the results shown at the low end of the temperature range.

5. Conclusions

A method to determine the coefficient of thermal dependence for Young's modulus of elasticity for aluminum 6061-T651 beams has been presented. The method is based upon acquiring the acoustic emission from the surface of an impacted beam under applied thermal loads. The shift in resonance due to the thermal load was then tracked. In this regard, MEMS microphones were employed for obtaining the resonance frequencies of the modally excited aluminum beam. The 5th natural frequency, obtained for *free-free* boundary support conditions, was used to extract the coefficient of thermal dependence for Young's modulus experimentally. This value was then employed in the theoretical model and compared to the experimental results obtained for the 2nd, 3rd and 4th natural frequencies. The theoretical results were in very good agreement with the experimental results obtained. Constant geometry and constant elasticity models were also presented in which it was determined that the elastic modulus is much more temperature sensitive

than the changes to the material geometry under the applied thermal load. Also, it was found that the thermal sensitivities of these two parameters were greater for temperatures above 21°C than for temperatures below 21°C.

References

[1] R. Braun, Effect of thermal exposure on the microstructure, tensile properties and the corrosion behaviour of 6061 aluminium alloy sheet, Materials and Corrosion 56 (2005) 159-165.

[2] Aerospace Specification Metals Inc. (2008), Material Data Sheet, Aluminum 6061 T6; 6061-T651.

[3] Aircraft Spruce & Specialty Co. (2008), General Aluminum Information Data Sheet, www.aircraftspruce.com.

[4] All Metals & Forge (2008), Product Description Sheet, Aluminum 6061, www.steelforge.com.

[5] McMaster-Carr Supply Company (2009), Product Data Sheet 8975KAC, www.mcmaster.com.

[6] M. R. Shankar, S. Chandrasekar, A. H. King, W. D. Compton, Microstructure and stability of nanocrystalline aluminum 6061 created by large strain machining, Acta Materialia 53 (2005) 4781-4793.

[7] J. K. Kim, H. K. Kim, J. W. Park, W. J. Kim, Large enhancement in mechanical properties of the 6061 Al alloys after a single pressing by ECAP, Scripta Materialia 53 (2005)1207-1211.

[8] J. C. Huang, C. S. Shin, S. L. I. Chan, Effect of temper, specimen orientation and test temperature on tensile and fatigue properties of wrought and PM AA6061-alloys, International Journal of Fatigue 26 (2004) 691-703.

[9] T. S. Srivatsan, S. Sriram, C. Daniels, Influence of temperature on cyclic stress response and fracture behaviour of aluminum alloy 6061, Engineering Fracture Mechanics 56 (1997) 531-550.

[10] Engineers Edge (2008), Aluminum Tempers Data Sheet, www.engineersedge.com.

[11] J. Amritsar, I. Stiharu, M. Packirisamy, Bioenzymatic detection of troponin C using micro-opto-electro-mechanical systems, Journal of Biomedical Optics 11 (2006) 021010-1-7.

[12] A. Chandrasekaran, G. Rinaldi, M. Packirisamy, Label-free detection of enzymatic interaction through dynamic behavior of microstructures, ICMEMS 2009 International Conference on MEMS, Chennai, India (2009) January 3-5.

[13] M. Su, S. Li, V. P. Dravid, Microcantilever resonance-based DNA detection with nanoparticle probes, Biochemical and Biophysical Research Communications 304 (2003) 98-100.

[14] R. Riesenberg, G. Nitzsche, A. Wuttig, B. Harnisch, Micro Spectrometer and MEMS for Space, 6th ISU Annual International Symposium, Smaller Satellites: Bigger Business, Strasbourg, France, (2001) May 21-23.

[15] V. K. Varadan, V. V. Varadan, Microsensors, Microelectromechanical Systems (MEMS), and Electronics for Smart Structures and Systems, Smart Materials and Structures 9 (2000) 953-972.

[16] Knowles Acoustics (2006), Product Data Sheet, SiSonic Microphone SPM0102ND3 Series, www.knowles.com.

[17] H. Wu, M. Siegel, Correlation of accelerometer and microphone data in the “coin tap test”, IEEE Transactions on Instrumentation and Measurement 49 (2000) 493-497.

[18] P. Cawley, R. D. Adams, The mechanics of the coin-tap method of nondestructive testing, Journal of Sound and Vibration 122 (1988) 299-316.

[19] C. M. Harris, C. E. Crede (1976), Shock and Vibration Handbook, McGraw-Hill Book Company, ISBN 0-07-026799-5, pages 1-14.

[20] G. Rinaldi, M. Packirisamy, I. Stiharu, An improved method for predicting microfabrication influence in atomic force microscopy performances, International Journal of Nanotechnology 1 (2004) 292-306.

[21] C. W. de Silva (2005), Vibration and Shock Handbook. Mechanical Engineering Series, ed. F. Kreith. Boca Raton, FL: Taylor and Francis Group, LLC 1872, 4-26-4-49.

[22] P. Davidson, R. Davis, Mechanical behavior of 6061-T651 aluminum, AIAA Journal 13 (1975) 1547-1548.

[23] W. R. Martin, J. R. Weir, Mechanical properties of X8001 and 6061 aluminum alloys and aluminum-base fuel dispersion at elevated temperatures, ORNL, Oak Ridge, Tennessee, USA (1964).

[24] F. Augereau, D. Laux, L. Allais, M. Mottot, C. Caes, Ultrasonic measurement of anisotropy and temperature dependence of elastic parameters by a dry coupling method applied to a 6061-T6 alloy, Ultrasonics 46 (2007) 34-41.

[25] G. Rinaldi, M. Packirisamy, I. Stiharu, Boundary characterization of microstructures through thermo-mechanical testing, Journal of Micromechanics and Microengineering 16 (2006) 549-556.

[26] G. M. Owolabi, A. G. Odeshi, M. N. K. Singh, M. N. Bassim, Dynamic shear band formation in aluminum 6061-T6 and aluminum 6061-T6/Al_2O_3 composites, Materials Science and Engineering 457 (2007) 114-119.

[27] S.-G. Kang, M.-G. Kim, C.-G. Kim, Evaluation of cryogenic performance of adhesives using composite-aluminum double-lap joints, Composite Structures 78 (2007) 440-446.

[28] Y. B. Guo, Q. Wen, M. F. Horstemeyer, An internal state variable plasticity-based approach to determine dynamic loading history effects on material property in manufacturing processes, International Journal of Mechanical Sciences 47 (2005) 1423-1441.

[29] G. Arfken, (1985), Mathematical Methods for Physicists, 3rd ed. Orlando, FL, USA, Academic Press.

List of symbols/abbreviations/acronyms/initialisms

a	support boundary sensitive variable (mode shapes)
a_1	arbitrary value
a_2	arbitrary value
A	n x n matrix (n >1)
AU	arbitrary units
b	support boundary sensitive variable (mode shapes)
B	n x 1 column matrix (n >1)
c	support boundary sensitive variable (mode shapes)
cm	centimeter
CTE	coefficient of thermal expansion
CTY	coefficient of thermal dependence for Young's modulus
d	support boundary sensitive variable (mode shapes)
DNA	deoxyribonucleic acid
E	Young's modulus of elasticity
E^*	normalized Young's modulus
G	geometry
GPa	giga-Pascal
h	thickness
Hz	Hertz
f_i	frequency (Hz)
K	elasticity
kHz	kilohertz
kg	kilogram
K_R	rotational spring constant
K_T	translational spring constant
K_R^*	normalized rotational spring constant
K_T^*	normalized translational spring constant
L	length
m	meter
MEMS	micro-electro-mechanical-systems
mm	millimeter

MPa	mega-Pascal
nm	nano-meter
Pa	Pascal
T	temperature
(T)	temperature dependent
V*	normalized volume
VDC	direct-current voltage
x	normalized length coordinate
XXXX	four digit index system (aluminum industry)
y	n x 1 column matrix (n >1)
y_1	undetermined coefficient
y_2	undetermined coefficient
y_3	undetermined coefficient
y_4	undetermined coefficient
y_5	undetermined coefficient
y_6	undetermined coefficient
$Y(x)$	flexural mode shape (deflection)
Δh	change in thickness
ΔL	change in length
Δw	change in width
ΔT	change in temperature
ΔE	change in Young's modulus
α_i	mode shape variable (boundary support dependent)
λ_i	eigenvalues
Λ	positional length coordinate
μ	micro
μm	micro-meter
ρ	material density
ρ*	normalized material density
~	approximately
°C	degrees centigrade
>	greater than
<	less than
∞	infinity

Distribution list

Document No.: DRDC Atlantic TM 2009-080

LIST PART 1: Internal Distribution by Centre:

1 DG / DRDC Atlantic
1 H / AVRS
7 AVRS
5 DRDC Atlantic Library

14 TOTAL LIST PART 1

LIST PART 2: External Distribution by DRDKIM

National Defence Headquarters
101 Colonel By Drive
Ottawa, ON
K1A 0K2
1 DRDKIM
1 Assoc, DGRDP
1 DSTA
1 DTAES
1 DTAES 7
4 DTAES 7-7
1 Library & Archives Canada, Attn: Military Archivist Government Records Branch

10 TOTAL LIST PART 2

24 TOTAL COPIES REQUIRED

This page intentionally left blank.

DOCUMENT CONTROL DATA

(Security classification of title, body of abstract and indexing annotation must be entered when the overall document is classified)

1. ORIGINATOR (The name and address of the organization preparing the document. Organizations for whom the document was prepared, e.g. Centre sponsoring a contractor's report, or tasking agency, are entered in section 8.)

DRDC Atlantic AVRS
9 Grove Street
Dartmouth, NS B2Y 3Z7

2. SECURITY CLASSIFICATION (Overall security classification of the document including special warning terms if applicable.)

UNCLASSIFIED

3. TITLE (The complete document title as indicated on the title page. Its classification should be indicated by the appropriate abbreviation (S, C, R or U) in parentheses after the title.)

MEMS Based Acoustic Thermomechanical Characterization of Aluminum 6061-T651 Beams

4. AUTHORS (last name, followed by initials – ranks, titles, etc. not to be used)

Rinaldi, G.

5. DATE OF PUBLICATION (Month and year of publication of document.)

September 2009

6a. NO. OF PAGES (Total containing information, including Annexes, Appendices, etc.)

48

6b. NO. OF REFS (Total cited in document.)

29

7. DESCRIPTIVE NOTES (The category of the document, e.g. technical report, technical note or memorandum. If appropriate, enter the type of report, e.g. interim, progress, summary, annual or final. Give the inclusive dates when a specific reporting period is covered.)

Technical Memorandum

8. SPONSORING ACTIVITY (The name of the department project office or laboratory sponsoring the research and development – include address.)

Defence R&D Canada - Atlantic
PO Box 1012
Dartmouth, NS B2Y 3Z7

9a. PROJECT OR GRANT NO. (If appropriate, the applicable research and development project or grant number under which the document was written. Please specify whether project or grant.)

9b. CONTRACT NO. (If appropriate, the applicable number under which the document was written.)

10a. ORIGINATOR'S DOCUMENT NUMBER (The official document number by which the document is identified by the originating activity. This number must be unique to this document.)

DRDC Atlantic TM 2009-080

10b. OTHER DOCUMENT NO(s). (Any other numbers which may be assigned this document either by the originator or by the sponsor.)

11. DOCUMENT AVAILABILITY (Any limitations on further dissemination of the document, other than those imposed by security classification.)

(X) Unlimited distribution
( ) Defence departments and defence contractors; further distribution only as approved
( ) Defence departments and Canadian defence contractors; further distribution only as approved
( ) Government departments and agencies; further distribution only as approved
( ) Defence departments; further distribution only as approved
( ) Other (please specify):

12. DOCUMENT ANNOUNCEMENT (Any limitation to the bibliographic announcement of this document. This will normally correspond to the Document Availability (11). However, where further distribution (beyond the audience specified in (11) is possible, a wider announcement audience may be selected.))

13. ABSTRACT (A brief and factual summary of the document. It may also appear elsewhere in the body of the document itself. It is highly desirable that the abstract of classified documents be unclassified. Each paragraph of the abstract shall begin with an indication of the security classification of the information in the paragraph (unless the document itself is unclassified) represented as (S), (C), (R), or (U). It is not necessary to include here abstracts in both official languages unless the text is bilingual.)

Temperature based testing is an important tool in determining the mechanical characteristics of structures. Metallic structures such as aluminum beams respond to high and low temperatures by expanding or contracting accordingly. Hence, the structure under goes changes in geometry that can influence its performance. Similarly, the elastic property of the material has a temperature dependence that contributes significantly to the overall mechanical qualities of the material. These thermally induced changes in geometrical and elastic parameters can be monitored through experimentation. In this work, a method based on flexural frequency response is described in which the variation in the experimental 5^{th} natural frequency under thermal loading is employed to extract the coefficient of thermal dependence of Young's modulus. This coefficient is then employed in the theoretical model to validate the experimental 2^{nd}, 3^{rd}, 4^{th} and 5^{th} natural frequencies of the aluminum beam. A micro-electro-mechanical-systems based microphone is used to monitor the frequency response of the vibrating beam. The theoretical model is based on a *free-free* boundary supported beam from which the natural frequencies are obtained. Constant geometry and constant elasticity models are also presented and compared. For demonstration purposes the proposed method is applied to an aluminum 6061-T651 beam. Experimental results are good agreement with the theoretical formulation.

14. KEYWORDS, DESCRIPTORS or IDENTIFIERS (Technically meaningful terms or short phrases that characterize a document and could be helpful in cataloguing the document. They should be selected so that no security classification is required. Identifiers, such as equipment model designation, trade name, military project code name, geographic location may also be included. If possible keywords should be selected from a published thesaurus, e.g. Thesaurus of Engineering and Scientific Terms (TEST) and that thesaurus identified. If it is not possible to select indexing terms which are Unclassified, the classification of each should be indicated as with the title.)

Aluminum 6061-T651, thermomechanical testing, frequency response, Young's modulus, constant geometry, constant elasticity, MEMS

This page intentionally left blank.

Defence R&D Canada

Canada's leader in defence
and National Security
Science and Technology

R & D pour la défense Canada

Chef de file au Canada en matière
de science et de technologie pour
la défense et la sécurité nationale

www.drdc-rddc.gc.ca